Pflügers Arch (1986) 406:397–404

Pflügers Archiv
European Journal of Physiology

The effect of temperature on Na currents in rat myelinated nerve fibres

Jürgen R. Schwarz

Physiologisches Institut der Universität Hamburg, UKE, Martinistrasse 52, D-2000 Hamburg 20, Federal Republic of Germany

Abstract. 1) Voltage clamp experiments were performed in single myelinated nerve fibres of the rat and the effect of temperature on Na currents was investigated between 0° C and 40° C.

2) The amplitude of the peak Na current changed with a $Q_{10} = 1.1$ between 40° and 20° C and with a $Q_{10} = 1.3$ between 20° and 10° C. Below 10° C the peak Na current changed with a $Q_{10} = 1.9$.

3) The temperature coefficient for time-to-peak (tp), the measure for Na activation, and τ_{h1} and τ_{h2}, the time constants for Na inactivation changed throughout the temperature range. Q_{10} for all of these kinetic parameters increased from 1.8–2.1 between 40° and 20° C to 2.6–2.7 between 20° and 10° C. Below 10° C Q_{10} increased to 3.7 for τ_{h1} and tp, and to 2.9 for τ_{h2}. When the series resistance artifacts were minimized by addition of 6 nM TTX, the Q_{10}'s at $T < 10$° C were 2.9–3.0.

4) When the temperature was decreased from 20° to 0° C, both the curve relating Na permeability to potential, $P_{Na}(V)$, and the steady state Na inactivation curve, $h_\infty(V)$, were reversibly shifted towards more negative potentials by 6 mV and 11 mV, respectively. When the temperature was increased from 20° to 37° C no shifts occurred.

5) The Hodgkin-Huxley rate constants $\alpha_h(V)$ and $\beta_h(V)$ were calculated from $h_\infty(V)$ and τ_h (or τ_{h1}) at 20° and 4° C. The shift in $h_\infty(V)$ and the change in $\tau_h(V)$, which occurred within this temperature range, could be described assuming a selective shift in $\beta_h(V)$ along the potential axis.

Key words: Node of Ranvier – Rat nerve – Na current – Temperature dependence – Voltage clamp

Introduction

Our knowledge of the temperature coefficients for Na conductance ($Q_{10} = 1.3–1.5$) and for the time constants of Na activation and inactivation ($Q_{10} = 2–3$) is based on studies in nerve fibres of cold-blooded animals, frog (Frankenhaeuser and Moore 1963; Moore 1971), squid (Hodgkin and Huxley 1952), and Myxicola (Schauf 1973). Most of these studies have been performed in a temperature range between 0° and 20° C. Little is known about the temperature dependence of mammalian nerve fibres and about the temperature dependence of Na currents at temperatures higher than 20° C. Therefore, one goal of the present study was the description of Na currents in mammalian nerve fibres within a large temperature range, between 0° and 40° C.

In mammals, the first voltage clamp experiments in single myelinated nerve fibres were performed by Horáckova et al. (1968) in the rat. They found, that these mammalian nodal membranes lack almost totally K currents. Since then, it was interesting to know, whether there are as well species differences between Na channels. Recently, detailed descriptions of the ionic permeabilities underlying the excitation process in rabbit and rat myelinated nerve fibres have been published. Chiu et al. (1979) as well as Brismar (1980) reported differences between the macroscopic Na currents of amphibian and mammalian nerve fibres. Their work suggested species differences on the single channel level. Others questioned this interpretation and referred the differences in the Na currents to differences in the series resistance, which is larger in mammalian than in amphibian nodes (Neumcke and Stämpfli 1982; Schwarz et al. 1985). All of these studies were performed near room temperature.

If species differences of Na channels would exist, they could as well exhibit different temperature dependences. Indications for such a difference have been reported by Chiu et al. (1979). In rabbit, they found a transition temperature at about 6° C for Na conductance and for the time constant of Na inactivation, whereas in frog nerve fibres they did not find a transition temperature. This is in contrast to findings of W. Schwarz (1979), who showed, that in frog nerve and muscle fibres a transition temperature for various kinetic parameters of Na permeability is present between 4° and 8° C.

In addition to a temperature dependent Q_{10}, several recent reports indicate a shift in both the $g_{Na}(V)$ curve and the $h_\infty(V)$ curve to more negative potentials when the temperature is decreased. In all of these studies the shift in $h_\infty(V)$ is larger than the shift in $g_{Na}(V)$ (Kimura and Meves 1979; Mrose and Chiu 1979). It will be shown, that shifts occur as well in rat nerve fibres. These shifts can be related to differences in the temperature dependence of the Hodgkin-Huxley rate constants of Na permeability.

Methods

Single myelinated nerve fibres (diameter 12–16 μm) were isolated from the sciatic nerve of adult albino rats (300–400 g, Sprague-Dawley). The procedure of dissection was similar to that described for amphibian nerve fibres (Stämpfli and Hille 1976). In this study only motor nerve fibres were used. The fibres were mounted in a recording chamber and a single node of Ranvier was voltage clamped as described by Nonner (1969). No compensated feedback was used to reduce the error produced by the resistance in

series with the nodal membrane. In order to block any K currents, the external solution superfusing the nodal membrane in compartment A contained 154 mM NaCl, 2.2 mM $CaCl_2$, 12 mM tetraethylammonium-chloride, 5 mM Tris (hydroxy-methyl)-aminomethane-HCl, and was adjusted to pH = 7.3. The internodes were cut in the side pools filled with a solution containing 155 mM CsCl and 5 mM NaCl.

Under voltage clamp the holding potential was adjusted to give a steady state Na inactivation h_∞ of approximately 0.7. This potential was assumed to be the normal resting potential of rat nerve fibres, $E_r = -78$ mV (Neumcke and Stämpfli 1982). All membrane potentials are given as deviations, V, from this holding potential, thus $V = E - E_r$, if not otherwise noted. The membrane currents were stored either on film or – after analog-to-digital conversion – on disc by a minicomputer (PDP 11/34).

The temperature of the solutions was changed by means of a Kryo-Thermostat and measured with a thermocouple in the immediate vicinity of the node under investigation in pool A. In order to exclude time-dependent effects, the temperature of the solutions was changed slowly (1°–2°C/min).

Na currents were calculated from the voltage drop across the resistance of the cut internode R_{ED} using a calibration factor of 32 MΩ (Brismar 1980). The time course of Na inactivation during a depolarizing pulse was, after subtraction of the leakage current, either determined from semilogarithmic plots of the Na current decay or by least squares fits using the following equation (see also Ochs et al. 1981):

$$I_{Na} = I'_{Na}/g \exp(-t/\tau_{h1}) + (1-g)\exp(-t/\tau_{h2})] . \quad (1)$$

The four adjustable parameters were: I'_{Na}, Na current which would be obtained by Na activation in the absence of Na inactivation, τ_{h1} and τ_{h2}, time constants of the fast and slow phase of Na current decay with their corresponding amplitude factors g and $(1-g)$. From the peak Na currents the Na permeability was calculated by the Goldman equation (see Frankenhaeuser 1960).

The temperature dependence of the Na current parameters was described by their temperature coefficient Q_{10}, which was determined from the equation:

$$Q_{10} = X_1/X_2^{[10/(T_2-T_1)]} \quad (2)$$

where X_1 is the value of the experimental parameter at the lower absolute temperature T_1, and X_2 is that at the higher absolute temperature T_2. The activation energy μ was determined from the equation

$$\mu = [RT_1T_2/(T_2-T_1)]\ln(X_2/X_1) \quad (3)$$

where R is the gas constant (8.314 JK^{-1} mol^{-1}).

If the temperature dependence of an experimental parameter X is given by $X(T) = A \exp(-\mu/RT)$, then the temperature coefficient and the activation energy are related by the equation (see Netter 1959, p. 557).

$$\ln Q_{10} = 10\,\mu/(T^2R + 10TR). \quad (4)$$

Results

1. General description

Membrane currents were recorded during a slow change in the temperature of the solution, usually beginning at an initial temperature of 20–25°C. Figure 1 shows two pairs of membrane currents, each recorded at 21° and 0°C. They were elicited with a depolarization of 60 mV with and without a prepulse of −45 mV. Cooling slowed the membrane current kinetics (note different time scales in Fig. 1) and reduced the amplitude of the peak currents. Peak current decreased more without a prepulse than with. From the peak Na currents, a steady state Na inactivation (h_∞) at V = 0 mV was calculated to be 0.70 at 21°C and 0.32 at 0°C. This decrease in h_∞ at $V = 0$ suggests a shift of the $h_\infty(V)$ curve to more negative potentials at 0°C.

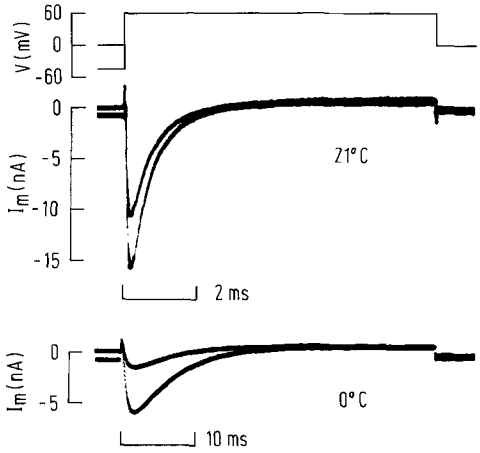

Fig. 1. Membrane currents recorded at 21° (*middle panel*) and 0°C (*lower panel*). At each temperature, membrane currents were elicited by a 60 mV depolarization with and without a 100 ms prepulse of −45 mV (see pulse programme in *upper panel*). Current traces photographically superimposed. K currents blocked by external TEA (10 mM) and internal CsCl. Leakage and capacity currents not subtracted. Note different time scales

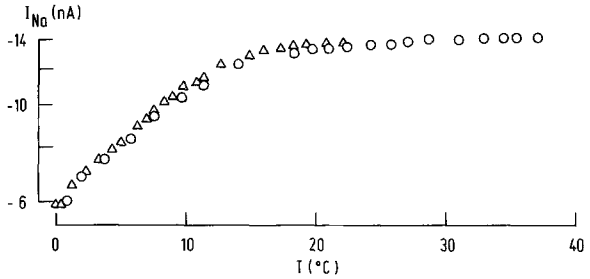

Fig. 2. Peak Na current semilogarithmically plotted versus temperature. The temperature was decreased from 22° to 0°C (△) and subsequently increased to 37°C (○). Rate of change in temperature ~1°C/min

Leakage current was barely affected by the change in temperature. This can be seen by comparing the amplitudes of the inward currents associated with the prepulses at the beginning of the current traces, as well as the amplitudes of the steady state outward currents. The latter were entirely leak currents, because K currents are normally very small in the rat (Brismar 1980; Brismar and Schwarz 1985) and in these experiments were blocked by external TEA and internal CsCl.

2. Peak Na current

Figure 2 shows a temperature dependent Q_{10} is present in rat myelinated nerve fibres. Peak Na currents were plotted

Table 1. Q_{10} values (mean ± SEM) for peak I_{Na}, kinetic parameters of I_{Na}, and duration of action potential, obtained from 12 fibres

	0°–10°C	10°–20°C	20°–30°C	30°–40°C
Peak I_{Na}	1.85 ± 0.09	1.32 ± 0.06	1.12 ± 0.06	1.12 ± 0.06
Time-to-peak	3.65 ± 0.17	2.73 ± 0.19	2.26 ± 0.22	1.83 ± 0.22
τ_{h1}	3.71 ± 0.16	2.64 ± 0.11	2.43 ± 0.22	2.06 ± 0.19
τ_{h2}	2.90 ± 0.27	2.71 ± 0.13	2.31 ± 0.19	1.99 ± 0.15
AP duration	3.66 ± 0.23	2.68 ± 0.04	2.20 ± 0.06	2.20 ± 0.06

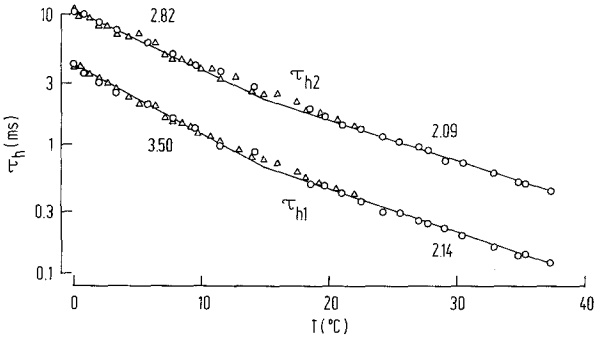

Fig. 3. Time constants of fast (τ_{h1}) and slow (τ_{h2}) phase of Na inactivation semilogarithmically plotted versus temperature. Same experiment and same change in temperature as in Fig. 2. The numbers next to the regression curves denote the Q_{10}

semilogarithmically versus temperature. In this experiment the temperature was decreased from 22° to 0°C and subsequently increased to 37°C. Despite a small "run-down" during the course of the experiment (about 60 min duration), the peak Na current recovered after rewarming. Within the upper ($T > 20$°C) and lower ($T < 10$°C) temperature ranges different straigth lines could clearly be fitted to the data. The Q_{10} was 1.85 at $T < 10$°C and 1.14 at $T > 20$°C. Between 10° and 20°C there is a curvinlinear relation between current and temperature. Similar results were obtained, when instead of peak I_{Na} the extrapolated I_{Na} at $t = 0$ were used.

In 11 experiments the Q_{10} changed gradually within this temperature range. Where possible, the data points between 10° and 20°C were fitted by a straight line as well. In order to describe the apparent differences in the temperature dependence, the entire temperature range was divided into four parts: 0°–10°C, 10°–20°C, 20°–30°C, and 30°–40°C. The Q_{10} values for peak I_{Na} were constant above 20°C, they are collected in Table 1.

The Q_{10} values for the amplitude of peak I_{Na} are influenced by the temperature dependence of the axoplasmic resistance R_{ED}, the Q_{10} being 1.22 between 10° and 25°C (Neumcke and Stämpfli, unpublished observation). Therefore, the "true" Q_{10} values for peak I_{Na} are larger by a factor given by the Q_{10} for R_{ED} in the rat, which, at the present, is unknown.

3. Activation and inactivation of Na currents

Development of Na inactivation in frog and rat nerve fibres is a diphasic process (Chiu 1976; Neumcke and Stämpfli 1982). In most experiments, the time constants τ_{h1} and τ_{h2} were determined from semilogarithmic plots of the Na current decay during the depolarizing test pulse (Chiu 1976; Kniffki et al. 1981). In a few fibres, least squares fits were determined using the mathematical model of Eq. (1) (Ochs et al. 1981). Both methods yielded similar results. The temperature dependence of Na activation was determined by the time-to-peak (tp). In Fig. 3, τ_{h1} and τ_{h2} were plotted versus temperature. The temperature dependence of these time constants and of the peak Na current (Fig. 2) in this and in other experiments did not exhibit an hysteresis as response to rewarming. Furthermore, Fig. 3 shows, that it is not possible to fit the data by single straight lines. In almost all experiments it seemed more adequate to determine the Q_{10} values in the four temperature ranges defined above. The Q_{10} values gradually decreased when the temperature was increased. The results of all experiments were collected in Table 1. It shows, that the largest change in Q_{10} occurred for τ_{h1} and tp near 10°C. This change in Q_{10} could simply be a reflection of the exponential relation between the temperature coefficient and the activation energy given in Eq. (4) (see Methods). With $\mu = 60$ kJ mol^{-1} and const. throughout the temperature range and with $Q_{10} = 2.0$ at 40°C, Eq. (4) predicts Q_{10} values for 20° and 0°C to be 2.20 and 2.41, respectively. This change in Q_{10} is smaller than that shown in Table 1.

In each experiment the amplitude factors of the fast and slow phase of Na inactivation showed a relatively large scatter. Nevertheless, the relative contribution of the slow phase to the total current amplitude was 0.15–0.30 above 15°–20°C and increased at lower temperatures in parallel with the decrease in the Na current amplitude. This is in accordance with the recent observation by Benoit et al. (1985) in frog nerve fibres.

The resistance in series with the nodal membrane has been reported to be larger in rat (440 kΩ; Neumcke and Stämpfli 1982) than in frog (220 kΩ; Drouin and Neumcke 1974). The series resistance and its effect on the time constants of Na activation and inactivation can be considered negligible, when the Na current amplitude is reduced to 30% (Neumcke and Stämpfli 1982). Accordingly, in the present experiments the influence of the series resistance on the time course of the Na current would change when the amplitude of the Na currents decreased during a decrease in the temperature below 15°C (see Fig. 1). In order to estimate the effect of the series resistance, three experiments were performed in the presence of 6 nM tetrodotoxin. Between 10° and 0°C the time constants of Na inactivation and the time-to-peak values yielded Q_{10} values of 3.0 for τ_{h1} and tp and of 2.9 for τ_{h2}. Thus, in the presence of TTX Q_{10} decreased for τ_{h1} and tp at $T < 10$°C, whereas Q_{10} for τ_{h2} remained unchanged. This result indicates, that at least part of the large change in Q_{10} at low temperature is induced by the relatively large series resistance in rat myelinated nerve fibres rather than by a phase transition of the membrane (discussed below). On the other hand, this finding demonstrates that the series resistance in rat nerve fibres plays an important role in the time course of the action potential. In six fibres, the temperature dependence of the action potential duration was found to closely parallel the Q_{10}'s of time-to-peak and τ_{h1} measured in the absence of TTX (see Table 1).

4. Shift of $P_{Na}(V)$ curve

Figure 4 shows $P_{Na}(V)$ curves, measured at three temperatures, in the order 22°, 0°, and 37°C. P_{Na} was calculated

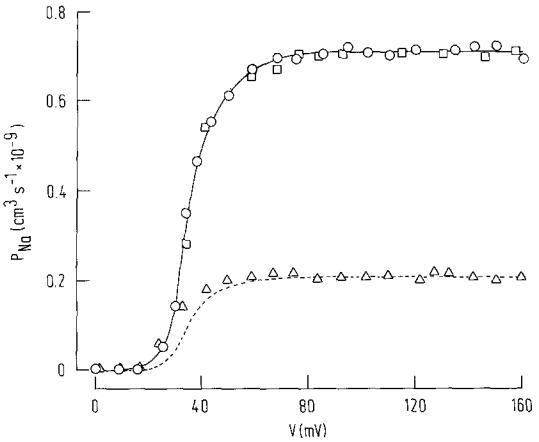

Fig. 4. Peak Na permeability plotted versus membrane potential V. The measurements were acquired in the following sequence: 20° (○), 0° (△), and 37°C (□). P_{Na} was calculated from the peak Na currents with the Goldman-Hodgkin-Katz equation (Frankenhaeuser 1960). A resting potential of $E_r = -78$ mV was assumed. *Smooth curve* through ○ was drawn by eye and scaled down to fit the maximum P_{Na} at 0°C (*dashed curve*). The curve fitting the P_{Na} values measured at 0°C (not shown) was shifted at the inflection point by 7 mV towards more negative membrane potentials. This shift was removed after temperature was increased to 37°C

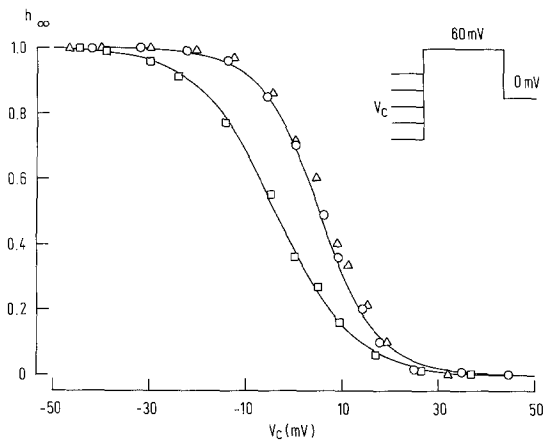

Fig. 5. Steady state Na inactivation curves. Sequence of measurements: 21° (○), 0° (□), and 37°C (△). *Smooth curves* represent least squares fits of the equation: $h_\infty = 1/[1 + \exp(V - V_h)/k]$ to ○ ($V_h = 5.15$ mV, $k = 6.21$ mV), □ ($V_h = -3.92$ mV, $k = 8.07$ mV), and △ ($V_h = 6.30$ mV, $k = 6.13$ mV, curve not shown). V_h, potential at which $h = 0.5$; k, slope factor. Inset, pulse programme; V_c, conditioning pulse

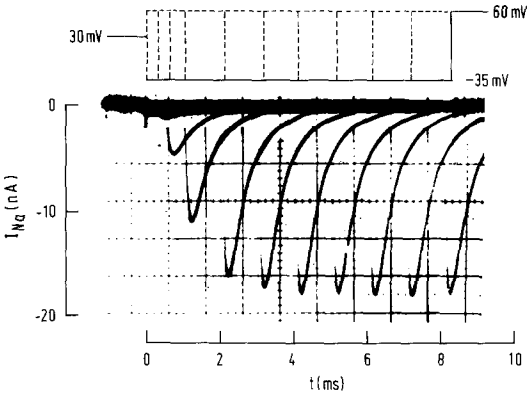

Fig. 6. Recovery from Na inactivation at 21°C. Oscilloscope records of membrane currents were superimposed. Na permeability was inactivated with a 100 ms pulse of 30 mV. Recovery from Na inactivation was traced with test pulses of 60 mV preceded by a pulse of −35 mV of increasing duration (see pulse programme in the *upper panel*)

from the peak Na currents with the Goldman-Hodgkin-Katz equation (Frankenhaeuser 1960) assuming an absolute resting membrane potential of $E_r = -78$ mV (Neumcke and Stämpfli 1982). Cooling caused a reduction of maximum peak P_{Na} from 0.70 to 0.21 $cm^3 s^{-1} \times 10^{-9}$. After rewarming there was no significant change in maximum P_{Na} at $T > 22°C$. This supports the finding of Brismar (1980), who observed the same maximum peak P_{Na} at 20° and 33°C. A consistent shift of the $P_{Na}(V)$ curve towards more negative potentials was found in five experiments. In order to demonstrate this shift, in Fig. 4 a smooth curve was fitted to the experimental data at 22°C and scaled down to fit the maximum P_{Na} at 0°C. The shift measured at the inflection point of the P_{Na} curves at 22° and 0°C in Fig. 4 was 7 mV, in five experiments with the same change in temperature, it was 5.5 ± 1.5 mV. The effect of a 440 kΩ series resistance upon the $P_{Na}(V)$ curve measured at 20°C would be a shift of about 3 mV to more positive potentials (Neumcke and Stämpfli 1982), therefore the corrected shift in $P_{Na}(V)$ at low temperatures is even larger than that observed.

5. *Shift of $h_\infty(V)$ curve*

The decreased steady state Na inactivation at the holding potential suggests a shift of the $h_\infty(V)$ curve towards more negative potentials when the temperature is decreased. Figure 5 shows $h_\infty(V)$ curves which were determined in the sequence 21°, 0°, and 37°C with the conventional double pulse protocol. When the temperature was lowered, the curve was shifted to the left by 9 mV and its steepness was decreased. The measured values were fitted to a Boltzmann equation of the form given by Hodgkin and Huxley (1952): $h_\infty = 1/(1 + \exp[(V - V_h)]$, where V_h denotes the inflection point and k (in mV) is the slope factor of the curve. Raising the temperature from 0 to 37°C reversed the shift, but there was no corresponding shift towards more positive potentials. In 12 fibres, decreasing the temperature from 20° to 0°C induced a reversible shift of 11.2 ± 1.3 mV (mean ± SEM) and a flattening of the curve, $k = 5.7 \pm 0.1$ mV at 20°C and $k = 6.8 \pm 0.2$ mV at 0°C. Increasing the temperature from 20° to 37°C, induced no significant shift. The error introduced by the series resistance upon the amount of shift in the $h_\infty(V)$ curve is < 1 mV, if the observed h_∞ values are corrected with Eq. (11) of the paper by Goldman and Schauf (1972).

6. *Temperature dependence of $\tau_h(V)$*

The time constants of Na inactivation within the potential range $-50 < V < 90$ mV were determined. Recovery from Na inactivation was measured at potentials $V \leqslant 0$ mV. One example is demonstrated in Fig. 6. Na permeability was inactivated with a 100 ms depolarizing pulse of 30 mV. Recovery from Na inactivation was traced at −35 mV with a test pulse of 60 mV after various time lags. The increase of

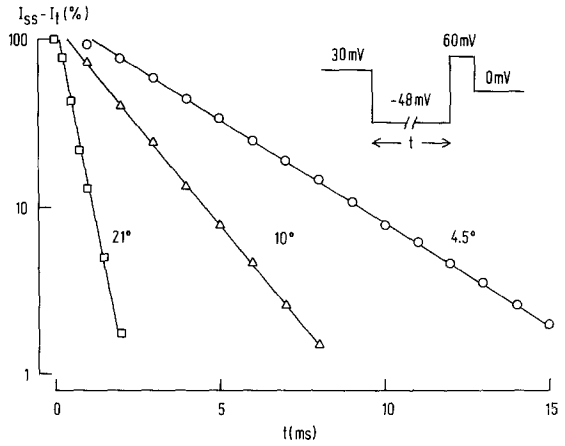

Fig. 7. Time course of recovery from Na inactivation at −48 mV at 21°, 10°, and 4.5° C. *Symbols* represent the differences (in %) between peak I_{Na} elicited after long prepulses (I_{ss}) and I_{Na} after shorter prepulse durations (I_t). Time constants calculated from the slope of the regression lines were 0.47 ms, 1.79 ms, and 3.09 ms, for 21°, 10° and 4.5° C, respectively

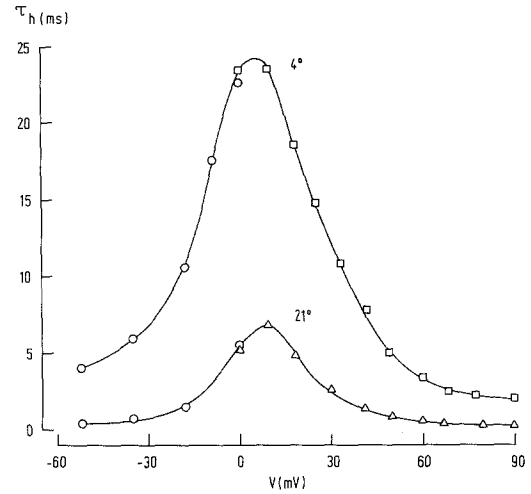

Fig. 8. Time constants of Na inactivation at 21° and 4° C plotted versus potential. Points at $V \leqslant 0$ mV were obtained from recovery experiments, points at $V \geqslant 0$ mV denote time constants obtained from development of Na inactivation (as described in the text). Smooth curves drawn by eye

the peak currents shown in Fig. 6 gives a measure of the time course. In rat, recovery from Na inactivation is very much the same as has been reported in frog (Chiu 1976).

Semilogarithmic plots of peak I_{Na} versus the duration of the prepulse of −48 mV are shown in Fig. 7 for 21°, 10°, and 4.5° C. The time course of recovery from Na inactivation could be fitted with one exponential plus an initial delay. Figure 7 shows, that there is a large temperature dependence of the initial delay. In three fibres, in which recovery from Na inactivation was measured at ten different temperatures between 4.5° and 21° C, the Q_{10} for this delay was 4.5, 5.0 and 5.3. Development of Na inactivation was traced with a three-pulse protocol at 0 mV < V < 30 mV, after removal of Na inactivation with a 100 ms pulse of −52 mV. At potentials V > 30 mV the time constants of development of Na inactivation were determined from the decay of the Na current.

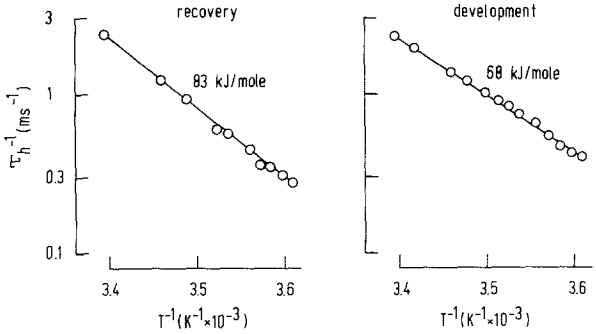

Fig. 9. Arrhenius plots. Reciprocals of Na inactivation time constants of recovery (*left*) and development (*right*) measured at −52 mV and 60 mV, respectively, plotted versus the reciprocals of absolute temperature. *Numbers* next to the *lines* denote activation energies (in kJ/mole)

Time constants of Na inactivation determined in one fibre at 21° and 4° C are shown in Fig. 8. The bell-shaped curves do not peak at the same potential, the peak of the curve measured at 4° C was shifted by 6 mV to more negative potentials relative to the curve measured at 21° C. The same was true in five similar experiments. The curves in Fig. 8 clearly show that there is not a single Q_{10} describing the temperature dependence of the time constants throughout the potential range. This was confirmed in experiments in which the time constants of Na inactivation were determined at two potentials where the reciprocals of the time constants represent the rate constants. Removal from Na inactivation at −52 mV and its development at 65 mV were measured at various temperatures between 21° and 4° C. An Arrhenius plot of the result of one experiment is shown in Fig. 9. The activation energy at −52 mV was 83 kJ/mole and at 65 mV it was 68 kJ/mole, corresponding to a Q_{10} = 3.90 and 2.79, respectively. The mean ± SEM of five experiments yielded a Q_{10} = 3.86 ± 0.07 at −52 mV and 2.80 ± 0.12 at 65 mV.

Discussion

The experiments show that in rat myelinated nerve fibres temperature dependent temperature coefficients exist for peak I_{Na} and for the kinetic parameters of Na activation and inactivation. When the temperature is increased from 0° to 40° C, Q_{10} gradually decreases. For peak I_{Na}, the largest change in Q_{10} occurs at about 10° C and is indicative of a transition temperature in rat nerve fibres. In addition, there are temperature dependent shifts in the $P_{Na}(V)$ and $h_\infty(V)$ curves: below 20° C they were reversibly shifted towards more negative potentials when the temperature was decreased, whereas above 20° C no shifts occurred. In the following these results are discussed and an interpretation of the shift in $h_\infty(V)$ is given.

A comparison of the present results in rat with those in rabbit nerve fibres given by Chiu et al. (1979) shows that there is a temperature dependent Q_{10} for Na conductance in both fibre types, but the Q_{10} values for Na conductance are quite different. In rat, Q_{10} for peak I_{Na} above 10° C has low values (Q_{10} = 1.1−1.3); in rabbit, Q_{10} for g_{Na} (as calculated from the extrapolated I_{Na} at t = 0) is larger (Q_{10} = 1.7), and describes g_{Na} between 6° and 40° C. In rabbit, at T < 6° C, a drastic increase of Q_{10} for g_{Na} to values as large as 4.7 occurs, whereas in the rat Q_{10} for peak I_{Na}

increases to only 1.9 below 10° C. This large difference in the Q_{10} for g_{Na} at low temperatures remains unexplained.

A temperature dependent Q_{10} for g_{Na} with a change at about 10° C has been reported in several preparations, e.g. in squid axons (Cole 1968; Kimura and Meves 1979) and in sheep Purkinje fibres (Dudel and Rüdel 1970). In contrast to mammalian myelinated nerve fibres, frog nerve fibres exhibit no temperature dependent Q_{10} for g_{Na} (Chiu et al. 1979).

The reduction of peak I_{Na} (or of g_{Na}) at low temperatures could be explained by a decrease in the number of Na channels or/and the single channel conductance. In nerve fibres, fluctuation analysis could help to decide between these alternatives, but have not as yet been performed at different temperatures. In other preparations, e.g. in chick myoballs (Fischbach and Lass 1978), noise experiments revealed a decrease in the single channel conductance with a transition temperature at 20° C. A decrease in the single channel conductance may also cause the decrease in I_{Na} in myelinated nerve fibres. In frog fibres, Sigworth (1980) reported a single channel conductance at 5° C to be 6.4 pS and $2-5\times10^4$ Na channels/node. Neumcke and Stämpfli (1983) found with a similar method, in the same preparation and at the same membrane potential, values of 13.4 pS and 4.2×10^4 Na channels/node at 15° C.

The occurrence of a transition temperature for g_{Na} has generally been interpreted as an indication of a phase transition of the membrane lipids. This change in the microenvironment of the integral channel proteins may lead to conformational changes of these proteins. In artificial membranes, with a single type of lipid, a distinct transition temperature has been observed (Chapman 1975). Biological membranes, on the other hand, are composed of a complex mixture of lipids, proteins, ions, and other components (Singer and Nicholson 1972). They would more likely show a gradual transition in the temperature function, as is present in the rat.

The Q_{10} values for the kinetics of Na current in rat are temperature dependent as well. This temperature dependence is larger than predicted from the exponential relation between temperature coefficient and activation energy [Eq. (4)]. The temperature dependent Q_{10} must be distinguished from the presence of a phase transition. Especially the experiments with TTX demonstrated, that part of the large change in Q_{10} for time-to-peak and τ_{h1} around 10° C, which at the first glance could be interpreted as an indication of a phase transition, was induced by the effect of the resistance in series with the nodal membrane. The large change in Q_{10} for τ_h reported by Chiu et al. (1979) may as well partly be induced by the series resistance, which in mammalian nerve fibres has been shown to be larger than in amphibian nerve fibres (Neumcke and Stämpfli 1982). Temperature dependent Q_{10} values for the gating processes of Na currents have also been reported in squid axons (Kimura and Meves 1979), whereas in amphibian nerve fibres Na current kinetics can be described with a single Q_{10}, if the temperature is changed only between 0° and 20° C (Chiu et al. 1979; Kniffki et al. 1981). On the other hand, when the frog preparation is cooled to such low temperatures as −6° C, W. Schwarz (1979) found transition temperatures for the time constants of Na currents between 4° − 8° C.

Traditionally, the decay of the macroscopic Na current is assigned to the inactivation process of Na channels (Hodgkin and Huxley 1952). Recently, Aldrich et al. (1983) have questioned this interpretation. In single channel recordings of neuroblastoma cells, they found that slow components of the activation process are rate limiting and are responsible for the macroscopic Na current decay, whereas Na inactivation, in their view, is fast and not dependent on voltage. Experiments in rabbit nerve fibres demonstrating a much faster Na current decay compared to that in frog (Chiu et al. 1979) seemed to support this different type of Na channel closing. Unfortunately, the present data about the temperature dependence of Na currents and the different amounts of temperature dependent shifts of the $P_{Na}(V)$ and $h_\infty(V)$ curves in rat fibres can not provide arguments in the discussion of this new interpretation. On the other hand, the present data can not support the notion, that there are differences between Na currents of mammalian and amphibian nerve fibres. This is in accordance with recent findings of Schwarz et al. (1985). They showed, that the kinetics of the Na current in rat fibres were altered by the effect of the series resistance. Na currents elicited with a 60 mV depolarization at 20° C were slowed by a factor of 1.3, when the Na current amplitude was decreased to 30% by 6 nM TTX.

Shifts of the $h_\infty(V)$ and $P_{Na}(V)$ curves occur when the temperature is decreased below 20° C. Cooling-induced shifts in $h_\infty(V)$ towards more negative potentials have also been reported in rabbit (Chiu et al. 1979) and frog nodes (Mrose and Chiu 1979; W. Schwarz, personal communication) as well as in squid axons (Wang et al. 1972; Kimura and Meves 1979). Several authors proposed that a shift in $h_\infty(V)$ may be explained by a difference in the Q_{10} for α_h and β_h. Such a difference is present in rat nerve fibres. Whether it can account for the shift in $h_\infty(V)$, shall now be discussed.

The rate constants α_h and β_h were calculated from the $h_\infty(V)$ curves and the time constants $\tau_h(V)$ from the equations given by Hodgkin and Huxley (1952): $\alpha_h = h_\infty/\tau_h$ and $\beta_h = (1-h_\infty)/\tau_h$. In this calculation it was assumed, that $\tau_h = \tau_{h1}$. In order to predict the $h_\infty(V)$ curve as well as the $\tau_h(V)$ curve at an unknown temperature, e.g. at 4° C, usually the appropriate rate constants are estimated from values at a given temperature, e.g. 20° C, with given Q_{10}'s. In the rat, Q_{10} for α_h determined at −52 mV is 3.9 and Q_{10} for β_h determined at 60 mV is 2.8. Assuming that the Q_{10}'s for both rate constants do not depend on potential, this difference in Q_{10} produces a shift in the $h_\infty(V)$ curve of only 5 mV towards more negative potentials, a value half that measured. Furthermore, within the potential range $-20\text{ mV} < V < 20\text{ mV}$, this difference in Q_{10} predicts time constants, which are considerably larger than those observed. On the basis of the data in the rat, one can therefore conclude that it is not possible to predict the $\tau_h(V)$ curve and the shift in $h_\infty(V)$ from the difference in Q_{10}.

Another way to explain the shift in the $h_\infty(V)$ curve is illustrated in Fig. 10. The symbols represent the rate constants α_h and β_h calculated from the $h_\infty(V)$ and $\tau_h(V)$ curves measured at 4° C. The continuous curves represent the predicted rate constants $\alpha_h(V)$ and $\beta_h(V)$, if a $Q_{10} = 3.9$ is assumed for both. Figure 10 shows that the predicted $\alpha_h(V)$ curve provides a good fit of the experimental data of α_h at 4° C. In order to achieve a fit for the β_h values at 4° C, the continuous curve was shifted by 12.5 mV towards more negative potentials (dashed curve). The same treatment with two other experiments yielded shifts of 12 and 13 mV, respectively. In all three experiments, a more satisfactory fit

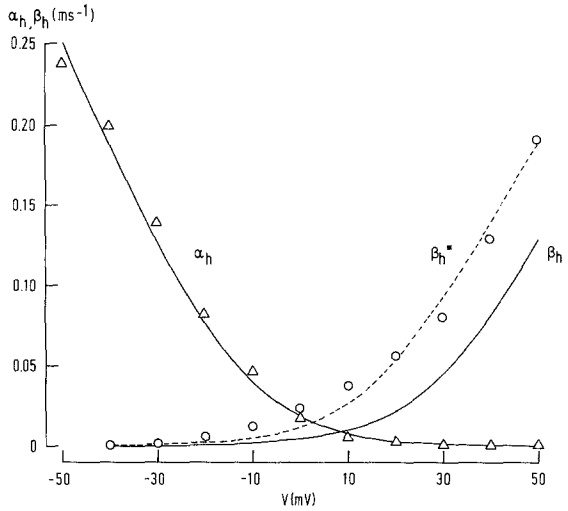

Fig. 10. Rate constants α_h (△) and β_h (○) measured at 4.5°C, plotted versus potential. *Smooth curves* represent least squares fits of the rate constants measured at 21°C, after division by a factor of 9.3 according to a $Q_{10} = 3.9$ for both. In addition $\beta_h(V)$ was shifted by 12.5 mV towards more negative potentials (β_h*; *dashed curve*)

of the β_h values measured at 4°C required a different slope of the $\beta_h(V)$ curve. In addition to a temperature dependent shift, this would indicate a voltage dependent Q_{10} for β_h. Voltage dependent Q_{10} values for the time constants of development of Na inactivation have also been reported in squid axons (Kimura and Meves 1979). This explanation of the shift in $h_\infty(V)$ proposes a different temperature dependence of the Hodgkin-Huxley rate constants describing the inactivation of Na channels. This should also be true in more complex models of Na inactivation (Chiu 1976). An equivalent description of the shift in the $P_{Na}(V)$ curve could not be performed with the present data, but a similar difference in the temperature dependence of the rate constants α_m and β_m could equally well explain the shift in $P_{Na}(V)$.

Several authors have tried to explain shifts in the $h_\infty(V)$ and $\tau_h(V)$ curves by a selective alteration of one rate constant. The shifts induced by a reduction in the extracellular pH could be reproduced by a selective increase in α_h (Courtney 1979). Another example is the shift in $h_\infty(V)$ and the induction of a slow component in the recovery from Na inactivation by phenobarbital. Both changes could be explained by a selective change in α_h (Schwarz et al. 1980). Rather than to speculate about an effect of temperature upon isolated parts of the Na channel macromolecule it is more attractive to think about mechanisms by which temperature could influence the structure of the membrane in a more general way. Temperature dependent changes in the fluidity have been discussed above. Another possible mechanism could be a change in membrane thickness. Haydon and coworkers (Haydon et al. 1980; Haydon and Kimura 1981; Haydon and Urban 1983) have put forward this hypothesis in order to explain the action of several lipophilic substances, like hydrocarbons. Hydrocarbons shift $h_\infty(V)$ and $m_\infty(V)$ similarly as has been described for a change in temperature. If these substances would be adsorbed in the nonpolar part of the membrane they could increase the membrane thickness and tension. A change in membrane thickness would change the electric field within the membrane experienced by the inactivation and activation voltage sensors (or those of the rate constants). It could be possible, that a change in temperature is also accompanied by a change in the thickness of the membrane. This idea is supported by observations in lipid-water systems. They show, that the thickness of the lipid phase decreases as the temperature is raised (see Luzzati 1968).

The temperature dependent changes in I_{Na} can explain phenomena, which are related to the reduced excitability at low temperature. E.g., if the temperature is decreased the conduction velocity is reduced until conduction block occurs, in mammalian myelinated nerve fibres at 7–9°C (Paintal 1965). Furthermore, at low temperatures, the depressing effect of impulse-blocking substances is stronger. This has been shown for allethrin (Wang et al. 1972) and benzyl alcohol (Harper et al. 1983). In addition to the reduction of the velocity of all physico-chemical reactions at a lower temperature the exaggerated effects can be explained by the reduction of the amplitude of the peak I_{Na} and by the shift of the $h_\infty(V)$ curve to hyperpolarizing potentials.

Acknowledgements. I thank Prof. B. Bromm for his continuous support and stimulating criticism and Prof. B. Neumcke and Dr. M. Leibowitz for valuable comments on the first draft of the manuscript. Financial support by the Deutsche Forschungsgemeinschaft is gratefully acknowledged.

References

Aldrich RW, Corey DP, Stevens CF (1983) A reinterpretation of mammalian sodium channel gating based on single channel recording. Nature (Lond) 306:436–441

Benoit E, Corbier A, Dubois J-M (1985) Evidence for two transient sodium currents in the frog node of Ranvier. J Physiol (Lond) 361:339–360

Brismar T (1980) Potential clamp analysis of membrane currents in rat myelinated nerve fibres. J Physiol (Lond) 298:171–184

Brismar T, Schwarz JR (1985) Potassium permeability in rat myelinated nerve fibres. Acta Physiol (Scand) 124:141–148

Chapman D (1975) Phase transitions and fluidity characteristics of lipids and cell membranes. Quart Rev Biophys 8:185–235

Chiu SY (1976) Inactivation of sodium channels: second order kinetics in myelinated nerve. J Physiol (Lond) 273:573–596

Chiu SY, Mrose HE, Ritchie JM (1979) Anomalous temperature dependence of sodium conductance in rabbit nerve compared with frog nerve. Nature (Lond) 279:327–328

Chiu SY, Ritchie JM, Rogart RB, Stagg D (1979) A quantitative description of membrane currents in rabbit myelinated nerve fibres. J Physiol (Lond) 292:149–166

Cole KS (1968) Membranes, ion and impulses. University of California Press, Berkeley Los Angeles

Courtney KR (1979) Extracellular pH selectively modulates recovery from sodium inactivation in frog myelinated nerve. Biophys J 28:363–368

Drouin H, Neumcke B (1974) Specific and unspecific charges at the sodium channels of the nerve membrane. Pflügers Arch 351:207–229

Dudel J, Rüdel R (1970) Voltage and time dependence of excitatory sodium current in cooled sheep Purkinje fibres. Pflügers Arch 313:136–158

Fischbach GD, Lass Y (1978) A transition temperature for acetylcholine channel conductance in chick myoballs. J Physiol (Lond) 280:527–536

Frankenhaeuser B (1960) Sodium permeability in toad nerve and in squid nerve. J Physiol (Lond) 152:159–166

Frankenhaeuser B, Moore LE (1963) The effect of temperature on the sodium and potassium permeability changes in myelinated nerve fibres of *Xenopus laevis*. J Physiol (Lond) 169:431–437

Goldman L, Schauf CL (1972) Inactivation of the sodium current in Myxicola giant axons. J Gen Physiol 59:659–675

Harper AA, MacDonald AG, Wann KT (1983) The effect of temperature on the nerve-blocking action of benzyl alcohol on the squid giant axon. J Physiol (Lond) 338:51–60

Haydon DA, Kimura JE (1981) Some effects of n-pentane on the sodium and potassium currents of the squid giant axon. J Physiol (Lond) 312:57–70

Haydon DA, Urban BW (1983) The action of hydrocarbons and carbon tetrachloride on the sodium current of the squid. J Physiol (Lond) 338:435–450

Haydon DA, Requena J, Urban BW (1980) Some effects of aliphatic hydrocarbons on the electrical capacity and ionic currents of the squid giant axon membrane. J Physiol (Lond) 309:229–245

Hodgkin AL, Huxley AF (1952) A quantitative description of membrane current and its application to conduction and excitation in nerve. J Physiol (Lond) 117:500–544

Horáckova M, Nonner W, Stämpfli R (1968) Action potentials and voltage clamp currents of single rat Ranvier nodes. Pro Int Union Physiol Sci 7:198

Kimura JE, Meves H (1979) The effect of temperature on the asymmetrical charge movement in squid giant axons. J Physiol (Lond) 289:479–500

Kniffki K-D, Siemen D, Vogel W (1981) Development of sodium permeability inactivation in nodal membranes. J Physiol (Lond) 313:37–48

Luzzati V (1968) X-ray diffraction studies of lipid-water systems. In: Chapman D (ed) Biological membranes. Academic Press, Orlando, pp 118–119

Moore LE (1971) The effect of temperature and calcium ions on the rate constants of myelinated nerve. Am J Physiol 221:131–137

Mrose HE, Chiu SY (1979) Is the steady-state inactivation curve for the sodium channel temperature dependent? Biophys J 25:193a

Netter H (1959) Theoretische Biochemie. Springer, Berlin Göttingen Heidelberg, p 557

Neumcke B, Stämpfli R (1982) Sodium currents and sodium-dependent fluctuations in rat myelinated nerve fibres. J Physiol (Lond) 329:163–184

Neumcke B, Stämpfli R (1983) Alteration of the conductance of Na channels in the nodal membrane of frog nerve by holding potential and tetrodotoxin. Biochim Biophys Acta 727:177–184

Nonner W (1969) A new voltage clamp method for Ranvier nodes. Pflügers Arch 309:176–192

Ochs G, Bromm B, Schwarz JR (1981) A three-state model for inactivation of sodium permeability. Biochim Biophys Acta 645:243–252

Paintal AS (1965) Block of conduction in mammalian myelinated nerve fibres by low temperatures. J Physiol (Lond) 180:1–19

Schauf CL (1973) Temperature dependence of ionic currents kinetics of Myxicola giant axons. J Physiol (Lond) 235:197–205

Schwarz JR (1984a) Rat myelinated nerve fibres exhibit a transition temperature for Na permeability properties. Pflügers Arch 400:R37

Schwarz JR (1984b) Different temperature coefficients of the rate constants α_h and β_h in rat nerve fibres. Pflügers Arch 402:R32

Schwarz JR, Bromm B, Ochs G (1980) Phenobarbital induces slow recovery from sodium inactivation of the nodal membrane. Biochim Biophys Acta 597:384–390

Schwarz JR, Neumcke B, Stämpfli R (1985) There is no difference in Na inactivation between rat and frog myelinated nerve. Pflügers Arch 405:R51

Schwarz W (1979) Temperature experiments on nerve and muscle membranes of frogs. Indications for a phase transition. Pflügers Arch 382:27–34

Sigworth FJ (1980) The variance of sodium current fluctuations at the node of Ranvier. J Physiol (Lond) 307:97–129

Singer SJ, Nicholson GL (1972) The fluid mosaic model of the structure of all membranes. Science 175:720–731

Stämpfli R, Hille B (1976) Electrophysiology of the peripheral nerve. In: Llinas R, Precht W (eds) Handbook of frog neurobiology. Springer, Berlin Heidelberg New York, pp 3–32

Wang CM, Narahashi T, Scuka M (1972) Mechanism of the negative temperature coefficient of nerve blocking action of allethrin. J Pharmacol Exp Ther 182:442–453

Received October 23/Accepted December 3, 1985